Strojnícky časopis – *Journal of* MECHANICAL ENGINEERING,
VOL 73 (2023), NO 2, 163 - 180

FRICTION STIR WELDING TOOL LIFE ASSESSMENT THROUGH FATIGUE ANALYSIS

TARAKA Hanuma[1], PARDEEP Pankaj[2], PANKAJ Biswas[3], ANILKUMAR Deepati[4*], INDIRA Benjeer[5], AADARSH Kumar[6]

[1, 2, 3] Indian Institute of Technology Guwahati, Department of Mechanical Engineering, Assam, India-781039
[4] CAIT, Department of Mechanical Engineering Technology, Jazan University, Jizan, Saudi Arabia-45142, e – mail: adeepati@jazanu.edu.sa*
[5, 6] GITAM University, Department of Mechanical Engineering, Visakhapatnam, Andhra Pradesh, India-530045

Abstract: Friction stir welding is a solid-state joining process used to weld various materials. Tool life is an important consideration when welding strong metals with the Friction stir welding technique (FSW). The current research aims to calculate tool life by mathematical derivation and simulation using ANSYS transient structural analysis. There are two tool materials and five-pin profiles to consider. The calculated tool life using mathematical formulation is within 15% of the simulation outcome. Further changes are made to the simulation to make the tool life estimate more realistic under FSW's operation. PcBN tool has superior mechanical properties over the tungsten carbide tool, so the procedure started with the tungsten carbide tool. The conical pin profile is giving 31466 cycles of tool life, which is 70 min run time while working at 450 rpm rotational speed. As a result, for high-strength materials joining, the tool must be chosen based on tool life parameters. The addition of a 1.5 mm fillet at the pin-to-shoulder junction has improved the tool life by 1147 cycles. The PcBN tool is simulated with a conical tool with new pin profiles of conical with grooves and cylindrical fillet with grooves. The maximum tool life of 94018 cycles is obtained for the conical PcBN tool.

KEYWORDS: finite element analysis (FEA), tungsten carbide, pcbn, tool life, simulation,

1 Introduction

Friction stir welding(FSW) has received enormous attention recently as a solid-state joining method for low-strength materials like Al and magnesium alloys. But it's now being tailored to the joining of potency and hard metals like stainless steel [1] . The technique involves spinning a tool plunged between two sheets that are closely abutted in a line along which the tool moves traversal. The frictional heat actuates as a result of the hard FSW tool rubbing on the workpiece softens and eventually joins the workpiece materials [2] . However, during the plunging period of joining high-strength materials, a significant amount of tool wear can be observed due to the generation of high heat input [3] . High forces are required in the FSW process for joining harder materials of high thickness may result in big and expensive machine tools [4] .

Most of the work related to the FSW is based on weld aspects only. All the effort of the development of technology is used to increase weld efficiency [5] , improve tensile strength [6] , fatigue strength

[7] , hardness, and material flow [8] , among other things. Several tests have been carried out to optimize process parameters based on tool failure. However, the impact of process factors on stress and moment detection is highly complex [9] . The most critical point in the FSW tool is certainly the surface attaching the shoulder to the pin. The critical circumference is equipped with several loads. Those are 1. Torque exerting due to rotation of pin inside the

DOI: 10.2478/scjme-2023-0031, Print ISSN 0039-2472, On-line ISSN 2450-5471

material, 2. A compressive force from the backing plate and shoulder, 3. Lateral and longitudinal forces due to material restoration [10] . All these forces combine to make the tool to failure. These forces are not the same during the entire FSW process. Sometimes, during the pin penetration itself, there can be a breakage of the tool [11] .

While observing the loads on the tool, it is evident that the tool is failing due to fatigue load. The load acting perpendicular to the pin profile is a transverse shear load (TSL) at a mid-point. Due to this TSL, a maximum reversed bending stress is acting at the pin-to-shoulder connecting surface. When the tool is enforced to break with the help of large process parameter values, the tool is broken at the same position. From the theoretical analysis and the past experimental results, a fatigue analysis of the tool needs to be done. The tool is not only affected by the stresses due to loads but also the temperature [12] . While joining the high-temperature and strength materials, the temperature at the stir zone is also maximum. The temperature effect on the tool has to be taken care of while determining the tool's life. The compatibility between the FSW tool and workpieces has a greater effect on the tool's life. So, there is a need of making that complex relationship between tool and workpiece materials based on tool life.

The tool material itself is the first thing to be noticeable in the FSW process. The tool materials like H13 tool die steels are primarily used for the joining of Al alloys at the start [13] . Gradually, the tool materials also evolved. The FSW process is rapidly improving day by day, and the necessity of different tool materials is also increasing rapidly. Tools for FSW applications such as metal matrix abrasive particles have higher demand [14] . In the mid-stages of development, titanium tools are procured because of having higher hardness and higher hot strength. The FSW is now developed and it can be useful for joining high-strength materials. Contemporarily, tungsten carbide (WC) and polycrystalline-boron-nitride (PcBN) are the primary tool materials employed to join high-strength materials [15] . All these tool materials discussed above are employed based on good weld characteristics but not from the tool life perspective.

Different types of tool pin profiles have been used for proper material mixing, fewer plunge forces, and ultimately good weld characteristics. Despite all these efforts by the tool, amidst the welding of high-strength materials such as low-carbon steel (LCS) and stainless steel(SS), severe abrasion was observed [16] . The tool pin geometry has a greater influence on the wear and breakage of the tool. Mastanaiah et al. (2018) and Biswas et al (2012) studied various effects of tool geometries on weld quality [17] . A hybrid tool pin is constructed with a conical threaded bottom and a triangular cross-section. This hybrid tool pin accelerates shear deformation and enhances workpiece material mixing and flow in the downward direction. Abhijit et al. (2020) determined the best pin profile for friction stir welding using an optimization method [18] . Tapered (T), taper threaded (TT), and cylindrical threaded (CT) tools were taken for the investigation, and concluded that taper threaded provides better welding characteristics. All the mentioned researchers have studied these hybrid pin profiles based on joint strength and other mechanical characteristics. None of them were studied based on the tool life perspective.

The experimental setup can be made to calculate the forces and moments acting over the tool [19] . Nevertheless, the calculation of the life of the tool using an experimental methodology is difficult. However, by using the data collected from the experimental setup and with the help of fatigue analysis in ANSYS, the fatigue life of the tool can be found. The same can be validated by using mathematical formulations. The entire study is done with the help of all available pin profiles working on the FSW process and tool materials related to high-strength material joining.

2 Methods and Methodology

2.1 Mathematical formulation for calculating tool life

The tool life is calculated by using experimental data. If there is any experimental data of loads acting on the tool by using the mathematical procedure, the tool life can be calculated. Various load leaps over tool pins are shown in Fig. 1. F_p and F_{sh} are the forces during tool plunging. F_t is the force during traversal. T is the entire torque on the tool pin and shoulder involved in the joining.

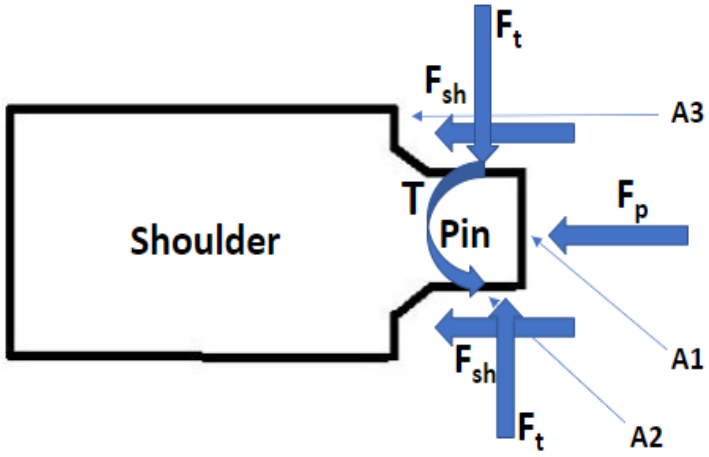


Fig. 1 Loads and areas of the FSW tool

A mathematical formulation will be useful to calculate the tool life using the strength of materials equations and

The total axial force on the tool = $F_p + F_{sh}$

Total force right-angle to tool axis = F_t

The torque acting on the pin = T

2.1.1 Assumptions

Assumptions:

1. The tool has enough rigidity to withstand all forces and moments.

2. The temperature effect will be considered by decreasing the strength of the tool.

To find out the tool life, the stresses induced in each part need to be calculated.

2.1.2 Axial stress

$$\text{Total axial force} = \mathrm{F_p} + F_{sh} \tag{1}$$

$$\frac{F_p}{F_{sh}} = \frac{A_{sh}}{A_p} = \frac{A3}{A1} \tag{2}$$

From equations (1) and (2) The forces can be calculated.

The stress values are given by

$$\sigma_p = \sigma_{sh} = \frac{F_p}{A_p} = \frac{F_{sh}}{A_{sh}} \quad (3)$$

2.1.3 Torsional shear stress

$$\text{Total area } A_t = A1 + A2 + A3 \quad (4)$$

The torques on each surface can be given as $T(\frac{A}{A_t})$.

The pin is more like to fail, therefore,

The total torque on the pin

$$T_p = T[(A1 + A2)/A_t] \quad (5)$$

The maximum torsional shear stress is given by

$$\tau = \frac{T_r}{J} = \frac{16T}{\pi d^3} \quad (6)$$

2.1.4 Bending stress due to Transverse load

Assuming the total load is acting over the midpoint on the circumferential area.

Maximum bending moment occurs at the root = $F_t(\frac{L}{2})$

This bending stress is completely reversed, and it is given as

$$\sigma_b = \frac{MY}{I} = \frac{32M}{\pi d^3} \quad (7)$$

2.1.5 Effect of Temperature

The maximum value of temperature can be calculated by inserting a thermocouple.

The influence of temperature and the ultimate strength of the tool is given by

$$(S_{ut})_T = (S_{ut})_{RT} * \left(\frac{S_T}{S_{RT}}\right)_T \quad (8)$$

where $(S_{ut})_T$ = The ultimate-tensile strength of the tool at maximum temperature provided by thermo-couple, $(S_{ut})_{RT}$ = The minimum ultimate tensile strength of the tool material at room temperature. $\left(\frac{S_T}{S_{RT}}\right)_T$ is the fraction to compensate for the effect of temperature by decreasing the ultimate tensile strength.

2.1.6 Calculation of endurance limit

$S_e^1 = 0.5 * (S_{ut})_T$ for steels, $S_e^1 = 0.4 * (S_{ut})_T$ for cast irons.

The endurance limit is given by

$$S_e = K_a * K_b * K_c * K_d * K_e * S_e^1 \quad (9)$$

where K_a is size factor, it depends upon the size of the component.

K_b is the surface finish factor.

K_c is load factor, the value is '1' for completely reversed bending, '0.7' for completely reversed axial load, and '0.6' for completely reversed torsion.

K_d is the reliability factor, '1' for 50% reliability.

K_e is modification factor = $\frac{1}{K_f}$.

2.1.7 Calculation of mean stress and stress amplitude

Based on the fillet radius, $\frac{D}{d}$ ratio, $\frac{r}{d}$ ratio the K_t value can be calculated. Notch sensitivity value is provided.

The fatigue sensitivity factor for bending $K_{fb} = 1 + q(K_t - 1)$.

Similarly, the same K_t, q values are calculated for an axial load.

The fatigue sensitivity factor for axial load $K_{fa} = 1 + q(K_t - 1)$.

Similarly, the same K_t, q values are chosen for torsion.

The fatigue sensitivity factor for torsion $K_{ft} = 1 + q(K_t - 1)$.

Only, the bending stress is fluctuating. Therefore, $(\sigma_a)_{bend}$ is only stress exists for stress amplitude calculation.

For mean stress calculation the axial stress, and torsional shear stress values are taken.

$$\sigma_a^1 = \{\left[K_{fb} * (\sigma_a)_{bend} + \left(K_{fa} * \frac{(\sigma_a)_{axial}}{0.85}\right]^2 + \left(3 * K_{ft} * (\tau_a)_{torque}\right)^2\right\}^{\frac{1}{2}} \quad (10)$$

$$\sigma_m^1 = \left\{\left[K_{fb} * (\sigma_m)_{bend} + K_{fa} * (\sigma_m)_{axial}\right]^2 + \left(3 * K_{ft} * (\tau_m)_{torque}\right)^2\right\}^{\frac{1}{2}} \quad (11)$$

If $\sigma_a^1 > S_e$, the tool is not having infinite life, the life will be definitely below 10^6 cycles. To find out the life pattern, the S-N curve is drawn.

For the life of 1000 cycles, the stress value is given as $0.9 * S_{ut}$

For the life of 10^6 cycles, the stress value is given as S_e

By plotting $LogS\ vs\ LogN$ curve, the tool life can be calculated.

2.2 Calculation of tool life using a mathematical model

The experimental data was gathered from published sources [20] . The tool's proportions are determined based on previous experience. The workpiece is made of AZ31B-O magnesium alloy, which has 2.5% to 3.5% Al, 0.7% to 1.3% Zn, and 0.2% to 1.0% Mn present in its composition. Tensile-strength UTS = 240 MPa, yield-strength = 140 MPa, elongation = 10%, and Young's modulus = 45 GPa are the characteristics. The weld plates considered were 200mm x 80mm x 5mm in size. To compute the forces, a length of 200 mm is necessary.

The tool is made of hot die steel(HDS). 1. Ultimate tensile strength(UTS) = 1200 -1590 MPa, yield strength = 1000-1380 MPa, melting point = 1427°C, young's modulus = 215GPa are the properties. The top diameter of the tool pin was 6 mm, the bottom diameter was 4 mm, and the pin length was 4.7 mm. The tool shoulder diameter was specified as about 15 mm. The process parameters were 300 mm/min to 500 mm/min rotational speed, 60 mm/min welding speed, 4.9 mm plunge depth, and a 2° backward tilt angle.

2.2.1 Experimental data

The experimental values,

The total axial force on the tool is reported as = $F_p + F_{sh}$ = 12.326 kN

Perpendicular to the tool axis, a total force F_t= 1.838 kN

Torque applied to the pin T = 19.66 kN.mm.

2.2.2 Axial stress

$F_P + F_{sh}$ = 12.326 kN

$\frac{F_p}{F_{sh}} = \frac{A_{sh}}{A_p} = \frac{A3}{A1}$. (Since $\sigma = F * A$)

$\frac{A_{sh}}{A_p} = \frac{\frac{\pi}{4}(15^2-5^2)}{\frac{\pi}{4}5^2} = \frac{200}{25} = 8.$

Therefore, F_p = 1.369 kN, F_{sh} = 10.956 kN

$$\sigma_p = \sigma_{sh} = \frac{F_p}{A_p} = \frac{1.369}{A_p} = 69.75 \text{ MPa} \approx 70 \text{ MPa}.$$

2.2.3 Torsional shear stress

$A1 = \frac{\pi}{4}5^2 = 19.634 \text{ mm}^2$

$A2 = \pi * 4.6 * 5 = 72.256 \text{ mm}^2$

$A3 = \frac{\pi}{4}(15^2 - 5^2) = 157.079 \text{ mm}^2$

Total area $A_t = A1 + A2 + A3 = 248.97 \text{ mm}^2$

The total torque on the pin $T_p = \frac{T(A1+A2)}{A_t} = \frac{19.66(19.634+72.256)}{248.97} = 7.256$ N. m.

The maximum torsional shear stress is calculated as follows:

$\tau = \frac{Tr}{J} = \frac{16T}{\pi d^3} = 16 * \frac{7.256}{\pi * 0.005^3} = 295.6411$ MPa ≈ 296 MPa.

2.2.4 Bending stress due to transverse load

The maximum bending moment at the root $= F_t\left(\frac{L}{2}\right) = 1.838\left(\frac{4.7}{2}\right) = 4.319$ N. m.

This bending stress is completely reversed,

$$\sigma_b = \frac{MY}{I} = \frac{32M}{\pi d^3} = 32 * \frac{4.319}{\pi * 0.005^3} = 351.968 \text{ MPa} \approx \pm 352 \text{ MPa}.$$

2.2.5 The effect of temperature

Considering, the maximum temperature developed = 400°C. The fraction as 0.9

Then $(S_{ut})_{400°C}$ = 0.9 × 1200 MPa = 1080 MPa.

2.2.6 Calculation of endurance limit

$$\sigma_p = 70 \text{ MPa}, \tau = 296 \text{ MPa}, \sigma_b = 352 \text{ MPa}.$$

$$S_e^1 = 0.5 * 1080 \text{ MPa} = 540 \text{ MPa}.$$

$$S_e = K_a * K_b * K_c * K_d * K_e * S_e^1 .$$

$$K_a = 4.51\,(1080)^{-0.265} = 0.708, \text{considering } K_b, K_c, K_d, K_e = 1$$

$$S_e = 0.708 * 540 = 382.57 \text{ MPa.}$$

2.2.7 Calculation of fatigue life

$(\sigma_m)_{bend} = 0.0, (\sigma_m)_{axial} = 70$ MPa, $(\tau_m)_{torque} = 296$ MPa.

$$\sigma_a^1 = \left\{\left[K_{fb} * (\sigma_a)_{bend} + \left(K_{fa} * \frac{(\sigma_a)_{axial}}{0.85}\right)\right]^2 + \left(3 * K_{ft} * (\tau_a)_{torque}\right)^2\right\}^{\frac{1}{2}}$$

= 1.3 * 352 = 457.6 MPa.

$$\sigma_m^1 = \left\{\left[K_{fb} * (\sigma_m)_{bend} + K_{fa} * (\sigma_m)_{axial}\right]^2 + \left(3 * K_{ft} * (\tau_m)_{torque}\right)^2\right\}^{\frac{1}{2}}$$

$$= \{[1.3 * 0 + (1.52 * 70)]^2 + 3 * (1.2 * 296)^2\}^{\frac{1}{2}} = 624.36 \text{ MPa.}$$

$\sigma_a^1 > S_e$, the tool is not having infinite life, the life will be definitely below 10^6 cycles. To find out the life pattern, the S-N curve is drawn.

For the life of 1000 cycles, the stress value is given as $0.9 * S_{ut}$ = 0.9 * 1080 = 972 MPa.

For the life of 10^6 cycles, the stress value is given as S_e = 382.57 MPa.

The fatigue life of the component $\text{Log}(S_f) = 3 + \left\{(6-3) * \left[\frac{2.987-2.66}{2.987-2.583}\right]\right\} = 5.226$

Therefore, the life of the component (N) = $10^{5.226} = 1.68 \times 10^5$

3 Calculation of tool life using finite element method

The material data was collected from the same source as the theoretical calculation data. The tool is made of hot die steel (HDS). 1. Ultimate tensile strength = 1200-1590 MPa, yield strength = 1000-1380 MPa, melting point = 1427°C, young's modulus = 215 GPa are the properties. The tool life is 1000 cycles for the S-N curve, and the strength is 0.9*0.9*1200 MPa. The factor '0.9' multiplied by strength accounts for the temperature effect. The strength of the infinite tool life is 382.57 MPa. For the material, linear interpolation of S-N curve data is used. The top diameter of the tool pin was 6 mm, the bottom diameter was 4 mm, and the pin length was 4.7 mm. The shoulder diameter of the tool was specified at 15 mm. The model was constructed in ANSYS 2020 using space claim, as illustrated in Fig. 2. The model has meshed into 5273 nodes and 2904 elements with a default element size (of 1.6229 mm). The meshed tool was depicted in Fig. 3.

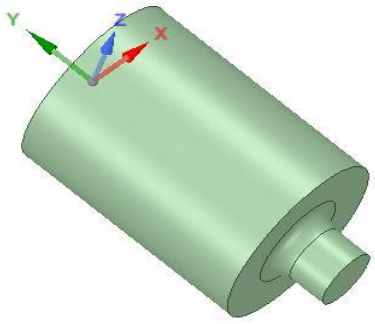


Fig. 2 FSW tool model

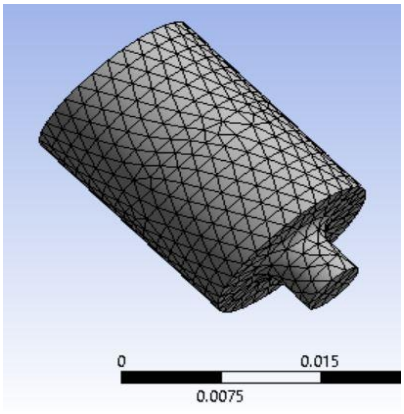


Fig. 3 FSW tool model

The loading on the tool is given the same as in theoretical calculation, total axial force on the pin = F_p = 1.369 kN, the force acting perpendicular to the pin axis F_t = 1.838 kN, the moment acting on the pin M = 7.246 kN.mm. The loading on the tool is shown in Fig. 4. The simulation was done for the calculation of the fatigue life of the tool. The von Mises stress values and deformation values are also calculated as part of the simulation. The life of the tool is shown in Fig. 5. The minimum tool life of the component from the mathematical model is 1.68×10^5 and from the simulation is 1.44×10^5. The % of error is below 15%. So, this simulation data can be useful to predict the actual tool life data.

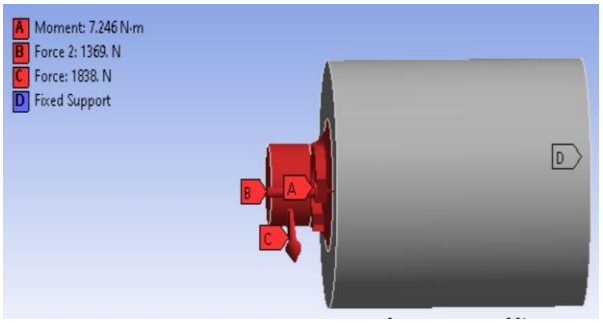


Fig. 4 Loading on the tool

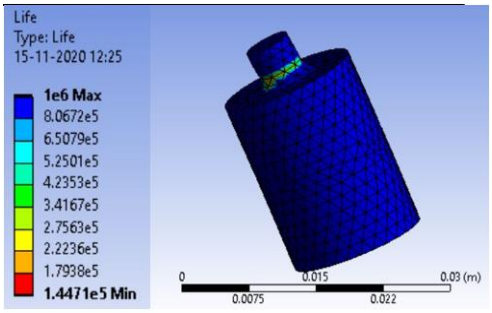


Fig. 5 Life of the tool

This procedure is having some limitations. This procedure is developed only based on a stage (i.e. traversal of the tool) of the entire FSW process. In the actual scenario, the FSW process consists of 4 stages. This procedure has to be extended to all 4 stages and the fatigue life will be cumulative of all 4 stages. some modifications to the procedure are mentioned here.

3.1 Modifications to the actual procedure of finite element method

The fatigue life of the FSW tool can be calculated by using the transient structural analysis in ANSYS software. In the previous technique of calculation of fatigue life, only the tool traversing phase is considered. But in the actual scenario, the entire technique is broken down into four steps in this procedure. Plunging, dwell, traversal, and ejection are the four options. Each step has a particular time and temperature range. For simulating each step, a particular time interval has to be taken from the experimental time. The temperature range is also taken as per the experimental results by using a thermocouple system. According to the load applied on the tool and temperature ranges, the entire process is segregated into different stages and is given below.

The entire process of FSW process is taken 55 seconds for the calculation of tool life. Stage 1,2,4 is of 10 seconds each and the main phase (i.e. traversal of the tool) takes 25 seconds of total working time. The selection of the tool is based on the fatigue tool life. For each stage, the fatigue life of the tool can be calculated by using transient structural analysis. The combined fatigue life of the tool can be calculated by using the miner's equation. Similar approaches of fatigue analysis and stress distributions on various manufacturing processes and weld joints studies are reported recently [21-22]

3.1.1 Fatigue life calculation

The fatigue life of the entire tool is determined using the miner's equation [23] and the notion of cumulative damage theory, as given below.

If a component is subjected to entirely reversed stresses ($\sigma 1$) for (n1) cycles, ($\sigma 2$) for (n2) cycles, and so forth, the miner's equation applies. If only the alternating stress ($\sigma 1$) is acting, one stress cycle will eat (1/N1) of the fatigue life, and since there are n1 such cycles at this stress level, the commensurate disruption to fatigue life will be [(1/N1) n1] or (n1/N1).

Correspondingly, at stress level $(\sigma 2)$, the corresponding damage will be (n2/N2). When these numbers are added together, we get

$$\frac{n1}{N1}+\frac{n2}{N2}+\frac{n3}{N3}+\cdots+\frac{nx}{Nx}=1 \tag{12}$$

Miner's equation is the equation seen above. Occasionally, the number of cycles n1, n2, At stress levels $\sigma 1, \sigma 2$, and so forth, results are uncertain. Assume that $\alpha 1, \alpha 2$, and so on are a percent of total life that will be eaten by stress levels $\sigma 1, \sigma 2$, and so on. Let N be the component's overall life. Then:

$$n1 = \alpha 1 N \tag{13}$$

$$n2 = \alpha 2 N \tag{14}$$

Substituting these values in the miner's Equation,

$$\frac{\alpha 1}{N1}+\frac{\alpha 2}{N2}+\cdots+\frac{\alpha x}{N3}=\frac{1}{N} \tag{15}$$

Also,

$$\alpha 1+\alpha 2+\alpha 3+\cdots+\alpha x=1 \tag{16}$$

In this procedure, the H13 tool is used to weld Al-Mg alloy. The life of the tool is in the order of 10^5 cycles. While joining high-strength materials like mild steel, and stainless steel the fatigue life of the tool may become in the order of 10^4 cycles. Therefore, the selection of the tool based on the tool's life comes into the picture. Tungsten carbide and PcBN tools are mostly used for the joining of high-strength materials. Using the help of simulation, various tool pin geometries can be applied to know the influence of probe geometry and tool material over tool life can be known.

Table 1. Loading on the FSW tool

	Cylindrical tool	**Tapered tool**	**Filleted tool**
Plunging pressure (MPa)	65.9	65.9	65.9
Pressure while traversal (MPa)	2.997×10^{-3}	3.008×10^{-3}	2.997×10^{-3}
Moment on pin bottom (N-mm)	3467	3205	3467
Moment on lateral pin sides (N-mm)	16277	9610	16277
Moment on shoulder	43866	16992	43866

Bottom (N-mm)			

4 Results and Discussion

4.1 FEA of tungsten carbide tool with different pin profiles

The forces and torques acting on the tool are measured utilizing dynamometer-based strain gauges was used [24] . The temperature distribution along the weld direction is measured using K-type thermocouples connected to the data acquisition system [25] . The tool used in this experiment is tungsten carbide and the workpiece material is stainless steel (304). This experiment is conducted at 470rpm and 60 mm/min traverse speed. The results of the simulation of the tool using fatigue analysis are comparably equal to the mathematical results. The tool pin profiles are selected from the regular usage of tools. Those are 1. cylindrical, 2. conical, and 3. cylindrical tool with fillet. From the experimental setup values of loads were found. The loads are divided based on the areas of their application. The values are shown in Table 1.

Table 2. The geometry and parameters of the FSW tools

Parameter	**Cylindrical tool**	**Tapered tool**	**Filleted tool**
Diameter of pin (mm)	7.9	7.9 - 5.71	7.9
Diameter shoulder (mm)	19	19	19
Height of pin (mm)	6.22	6.22	6.22
Axial pressure (MPa)	65.9	65.9	65.9
RPM of tool	450	450	450
Traversal speed (mm/s)	2	2	2
Radius of fillet(mm)	-	-	1.5
Thread pitch (mm)	-	-	-
Taper angle (^{o})	-	10	-

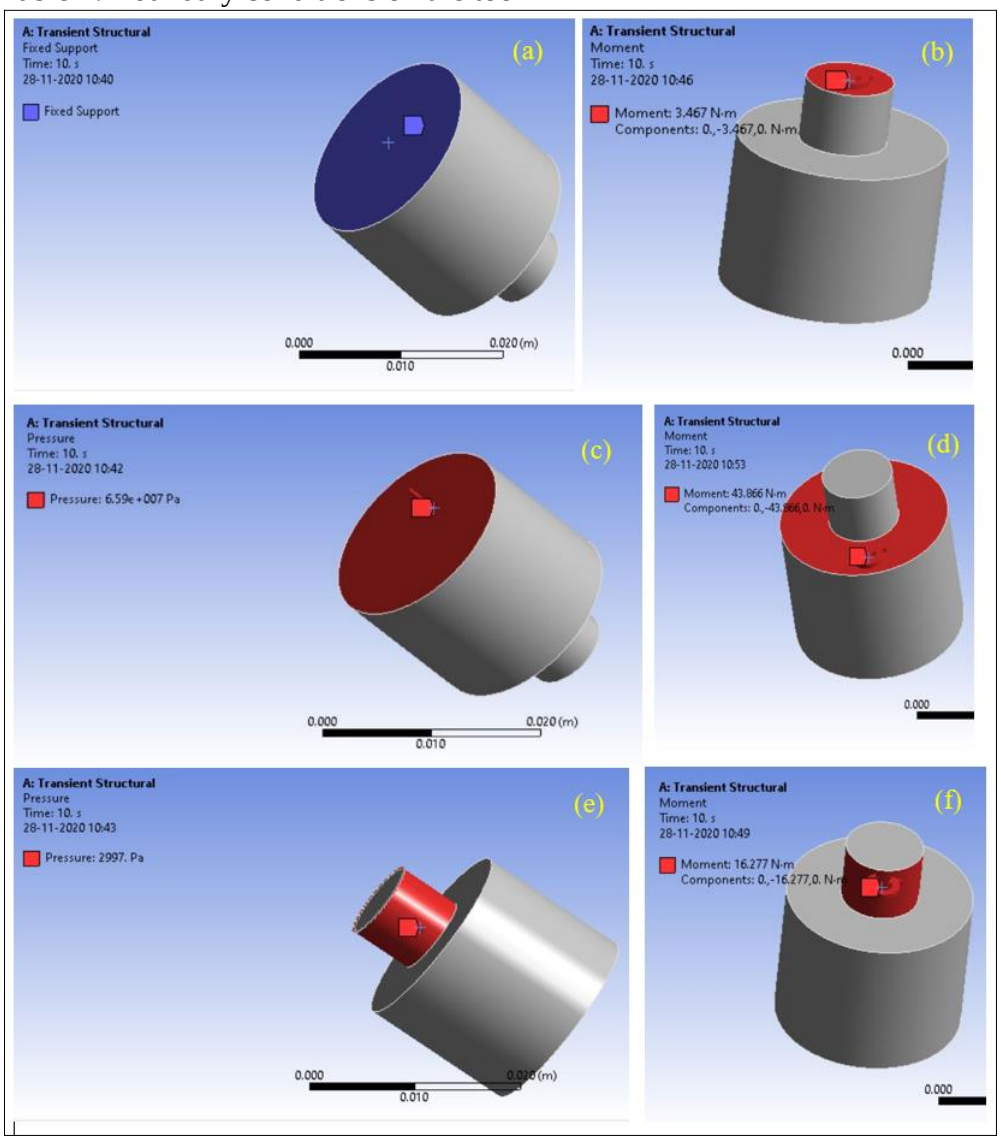
Table 3. Mechanical properties of the tool material (tungsten carbide)

Property	**Value**
Ductility	0.005
Bulk modulus (GPa)	350
Poisson’s ratio	0.2
Density (kg/m^3)	15250
Elastic limit (MPa)	335
Young’s modulus (GPa)	600
Hardness (MPa)	17000
Modulus of rupture (MPa)	482
Compressive strength (MPa)	3347
Shear modulus (GPa)	243
Tensile strength (MPa)	370
Fracture toughness (MPa.m$^{1/2}$)	2
Latent heat of fusion (kJ/kg)	330

Max service temperature (K)	1000
Specific heat (J/kg.K)	184
Thermal conductivity (W/m.K)	28
Thermal expansion (10^{-6}/K)	4.5

From the modifications to the actual procedure, all the stages won't be applied with all the loads. The loads are also varying with time. Therefore, transient structural analysis in ANSYS will be useful to simulate the data. The material properties and geometry of the tools are given here in Table 2, and Table 3 respectively.

Table 4. Boundary conditions on the tool



The boundary conditions are applied to all types of tool pin geometries. The values are changing based on the stage at which they were applied. All the boundary conditions are applied and shown in Table 4.

The fatigue life of the tool is given by how many rotations are undergone by the tool before failure. By using ANSYS simulation software by applying all the boundary conditions the tool life was calculated. The loads are selected based on their applicability at that stage. All stages have different tool life; by using the miner's equation the life can be calculated. Stage 1 and stage 3 are the main stages affecting the tool life. Stage 1 is the plunging of the tool into the workpiece resulting in more fatigue stress. While stage 4 is the plunging out the

tool always has 10^6 cycles. Stage 3 is an important phase, where the tool is having both traversal and rotational motions. The tool life of the different pin profiles is shown in Table 5. The values are tabulated in Table 6.

Table 5. The fatigue life of the different pin profiles

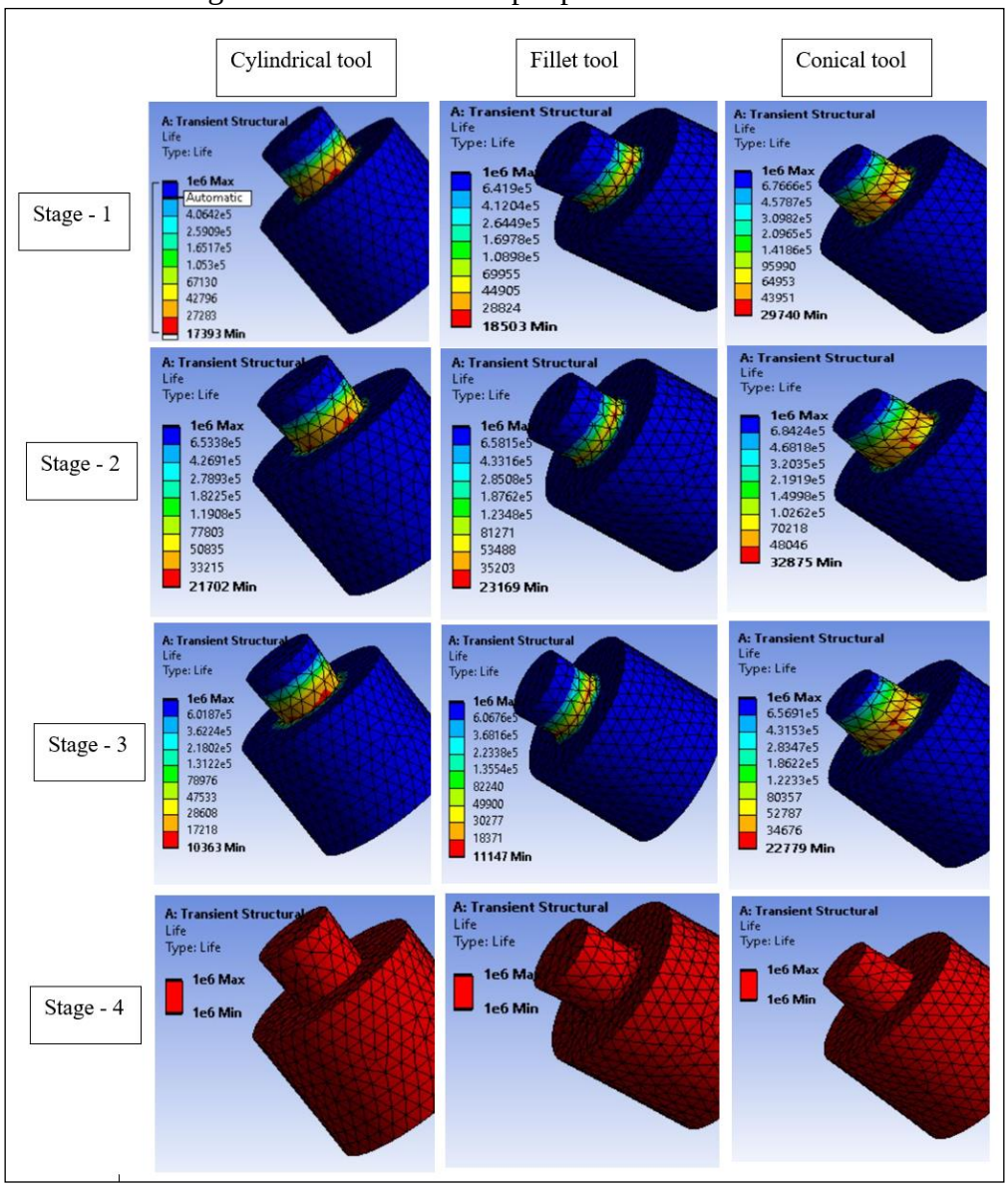


Table 6. Tool life in each stage

Tool life (No of cycles)	Cylindrical tool	Fillet tool	Conical tool
Stage - 1	17393	18503	29740
Stage - 2	21702	23169	32875
Stage - 3	10363	11147	22779
Stage - 4	10^6	10^6	10^6

The fatigue life of the tool is given by the miner's equation. In this estimation of fatigue life, the total working time of the tool is taken as 55 seconds. Stage 1, stage 2, and Stage 4 are of 10 seconds each and Stage 3 is of 25 seconds long. The conical tool has the highest fatigue life of 31466 cycles, and the cylindrical pin shape produces the lowest fatigue life of 15905 cycles. The fillet radius of 1.5 mm used in the cylindrical pin profile has improved the fatigue life by 1147 cycles. The fatigue life of the tool is given below in Table 7.

Table 7. Tool life

Tool life (No of cycles)	Cylindrical tool	Fillet tool	Conical tool
	15905.9	17052.6	31466

4.2 Finite element analysis of the PcBN tool with diverse pin profiles

PcBN is one of the known hardest tools for FSW of high-strength materials. The load values are taken the same as that of the tungsten carbide tool assuming no effect of tool material on welding loads, the forces are converted to pressures as they are acting normally on the surfaces. From the literature review on different pin profiles and based on the easiness of the flow of material 2 more pin profiles are taken into consideration. The addition of grooves makes the tool easy to move along the traverse direction. The previous study insisted that the tool with a conical pin profile is providing better tool life [26, 27]. Now the study is completely based on comparing the tool life of 3 tools. The 3 tools are 1. Conical, 2. conical with grooves 3. cylindrical fillet with grooves and are shown in

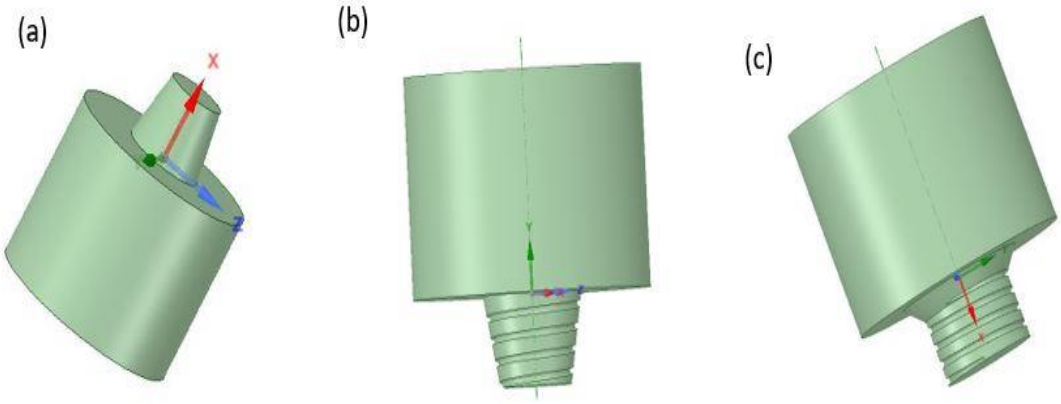


Fig. 6 Tool geometry with different pin profiles (a) conical tool (b) conical tool with grooves (c) cylindrical tool with fillet and grooves

The dimensions of the tool and the material properties of the PcBN tool are presented in Table 8 and Table 9 progressively.

Table 8. Dimensions of the tools

	Conical tool	Conical tool with grooves	Cylindrical tool with grooves
Diameter of pin (mm)	7.9 - 5.71	7.9 - 5.71	7.9
Diameter shoulder (mm)	19	19	19
Height of pin (mm)	6.22	6.22	6.22
Axial pressure (MPa)	65.9	65.9	65.9
RPM of tool	450	450	450

Traversal speed (mm/s)	2	2	2
Radius of fillet(mm)	-	-	1.5
Thread pitch (mm)	-	1.25	1.25
Taper angle (^{o})	10	10	-

Table 9. Material properties of the tool (PcBN)

Property	**Value**
Density (kg/m^3)	3100
Bulk modulus (GPa)	320
Poisson's ratio	0.145
Young's modulus (GPa)	680
Specific heat (J/kg.K)	184
Elastic limit (MPa)	855
Fracture toughness (MPa.m$^{1/2}$)	10
Hardness (MPa)	4000
Modulus of rupture (MPa)	615
Compressive strength (MPa)	4140
Max service temperature (K)	1370
Thermal expansion (10^{-6}/K)	4.9
Shear modulus (GPa)	297
Tensile yield strength(MPa)	965
Ductility	0.0045
Latent heat of fusion (kJ/kg)	330
Thermal conductivity (W/m.K)	100

The fatigue life of the tool is given by how many rotations are undergone by the tool before failure. By using ANSYS simulation software by applying all the boundary conditions the life was calculated. All stages have different tool life, by using the miner's equation the life can be calculated. Stage 1 and stage 3 are the main stages affecting the tool life. Stage 1 is the plunging of the tool into the workpiece resulting in more fatigue stress. While stage 4 is the plunging out the tool always has 10^6 cycles. Stage 3 is an important phase, where the tool is having both traversal and rotational motions. The fatigue life of the tool at different stages is shown in Table 10. and tabulated in Table 11.

The FSW tool fatigue life is given by the miner's equation. In this estimation of fatigue life, the total working time of the tool is taken as 55 seconds. Stage 1, stage 2, and Stage 4 are of 10 seconds each and Stage 3 is of 25seconds long. By using the miner's equation, the PcBN tool life is calculated and shown in Table 12. Here also, the tool with a conical pin profile is giving highest tool life of 94018.54 cycles.

The grooves added may have better material mixing, but according to the tool life perspective, the tool life is decreased by almost 30 percent. When comparing the tool life of Tungsten carbide and PcBN tools of the same pin profile (conical) a drastic change in tool life is observed. The conical tool of tungsten carbide is providing 31466 cycles. Under the same conditions, and pin profile PcBN tool is providing 94018 cycles. A total of 198 percent raise in tool life is observed.

CONCLUSIONS

With the collaborative efforts of mathematical modeling and finite-element analysis(FEA) data, the life of the tool is calculated.

- During the friction stir welding of strong, elevated re-crystallization temperature and high-strength materials, the tool life is suddenly decreased from the order 10^5 to 10^4 cycles.
- The total process of friction stir welding is divided into 4 stages. Stages 1,2,3 were provided comparably the same fatigue tool life. While in stage 4 tool is having infinite life.
- When comparing the fatigue tool life of the cylindrical tool, a cylindrical tool with fillet, and a conical tool. The conical tool pin provides better tool life of 31466 cycles.
- With the addition of a fillet of 1.5 mm radius to the cylindrical tool, the tool life has been improved by providing 1147 more cycles.
- The better tool (conical pin profile) is providing 31466 cycles. While the rotational speed used in this process is 450 rpm, that means the tool can have a life of 70 minutes. Therefore, there is a need for the selection of tools based on the tool life.
- The usage of PcBN material for the tool has significantly increased the tool life from 31466 cycles (Tungsten carbide tool with conical pin profile) to 94018 cycles (PcBN tool with conical pin profile).
- The effect of grooves on the tool pin perhaps be useful as a better material mixing point of view but from a tool life point of view, these grooves and surface profiles decrease the tool life.
- The tool life of a conical tool, a conical tool with grooves, and a cylindrical tool with grooves are 94018.54, 66264.22, and 45617.52 respectively.

Table 10. Life of the tool at different stages

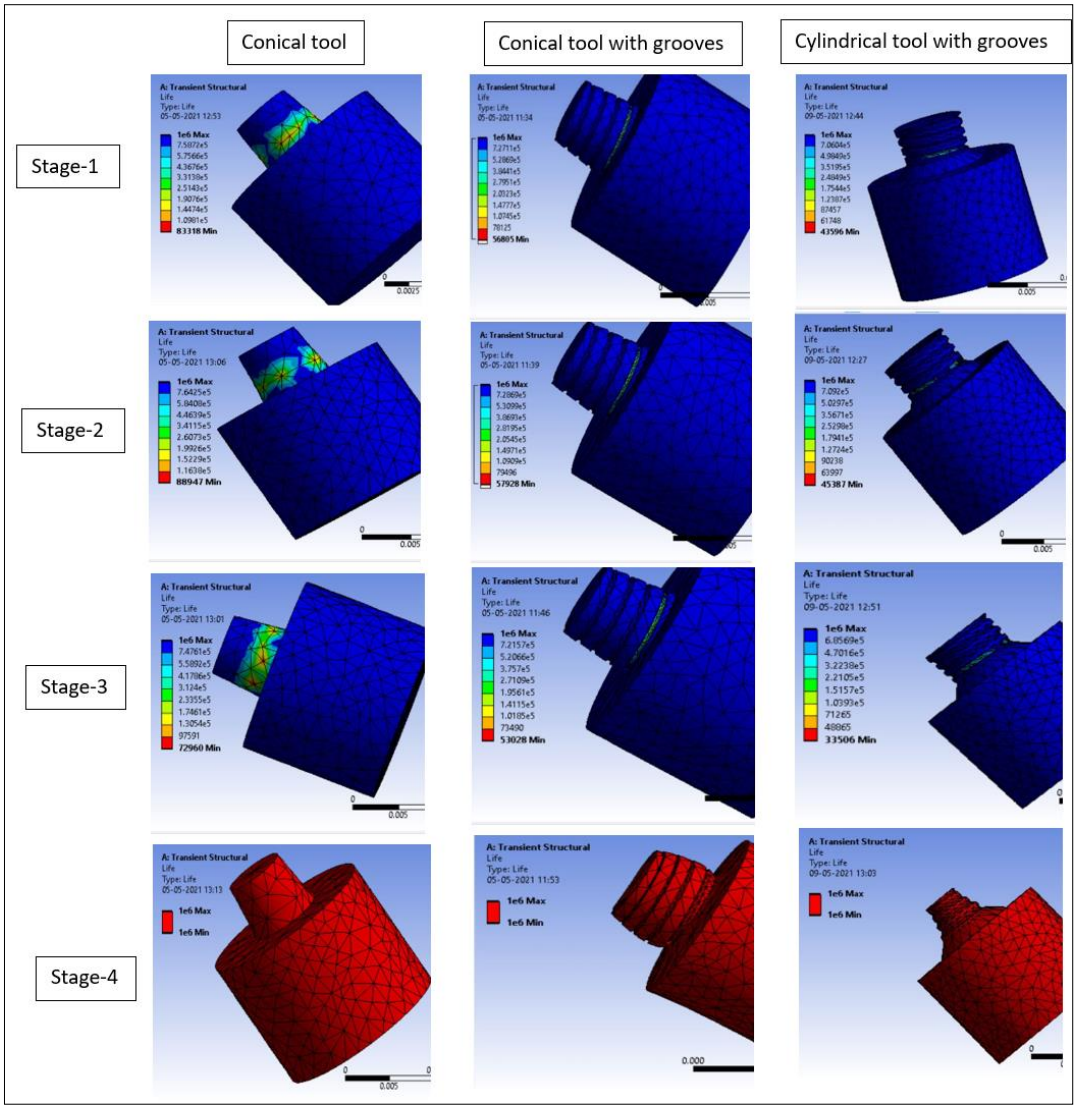


Table 11. Tool life at different stages

Tool life (No of cycles)	Conical tool	A conical tool with grooves	A cylindrical tool with grooves
Stage - 1	83318	56805	43596
Stage - 2	88947	57928	45387
Stage - 3	72960	53028	33506
Stage - 4	10^6	10^6	10^6

Table 12. Tool life of different pin profiles of PcBN

Tool life(No of cycles)	Conical tool	A conical tool with grooves	A cylindrical tool with grooves
	94018.54	66264.22	45617.52

References

[1] Thomas, W. M. "Friction Stir Butt Welding", International Patent Application No. PCT/GB92. GB Patent Application No. 9125978.8., **1991**.

[2] Chen, C.. Kovacevic, R. “Thermomechanical modelling and force analysis of friction stir welding by the finite element method”, Proceedings of the Institution of Mechanical Engineers, Part C: Journal of Mechanical Engineering Science 218(5), pp. 509 – 519, **2004**. DOI:10.1243/095440604323052292

[3] Tiwari, A., Pankaj, P., Suman, S., Singh, P., Biswas, P., Pal, S., Rao, A.G. “Effect of plasma preheating on weld quality and tool life during friction stir welding of DH36 steel”, Proceedings of the Institution of Mechanical Engineers, Part B: Journal of Engineering Manufacture, p. 0954405421990139, **2021**. DOI: 10.1177/ 0954405421990139

[4] Sinclair, P. C., Longhurst, W. R., Cox, C. D., Lammlein, D.H., Strauss, A. M. Cook, G. E. “Heated friction stir welding: an experimental and theoretical investigation into how preheating influences process forces”, Materials and Manufacturing Processes 25 (11), pp. 1283 – 1291, **2010**. DOI: 10.1080/10426914.2010.496122

[5] Deepati, A. K., Alhazmi, W., Zakri, W., Shaban, E., Biswas, P. “Parametric Analysis on the Progression of Mechanical Properties on FSW of Aluminum-Copper Plates”, Advances in Science and Technology Research Journal 16(2), pp. 168 – 178. 2022. DOI: 10.12913/22998624/147123

[6] Hattingh, D. G., Blignault, C., Van Niekerk, T. I. and James, M. N. “Characterization of the influences of FSW tool geometry on welding forces and weld tensile strength using an instrumented tool”, Journal of materials processing technology 203(1-3), pp. 46 – 57, **2008**. DOI: 10.1016/j.jmatprotec.2007.10.028

[7] Fratini, L., Buffa, G., Palmeri, D., Hua, J., Shivpuri, R. “Material flow in FSW of AA7075–T6 butt joints: numerical simulations and experimental verifications”, Science and Technology of Welding and Joining 11(4), pp. 412 – 421, **2006**. DOI: 10.1179/174329306X113271

[8] Emamian, S.S., Awang, M., Yusof, F., Sheikholeslam, M. Mehrpouya, M. “Improving the friction stir welding tool life for joining the metal matrix composites”, The International Journal of Advanced Manufacturing Technology 106(7), pp. 3217 – 3227, **2020**. DOI: 10.1007/s00170-019-04837-1

[9] Panneerselvam, K., Lenin, K. “Investigation on effect of tool forces and joint defects during FSW of polypropylene plate”, Procedia engineering 38, pp. 3927 – 3940, 2012. DOI: 10.1016/j.proeng.2012.06.450

[10] Balasubramanian, N., Gattu, B. Mishra, R. S. “Process forces during friction stir welding of aluminium alloys”, Science and technology of welding and joining 14(2), pp. 141 – 145, **2009**. DOI: 10.1179/136217108X372540

[11] Chen, C. M., Kovacevic, R. “Joining of Al 6061 alloy to AISI 1018 steel by combined effects of fusion and solid state welding”, International Journal of Machine Tools and Manufacture 44(11), pp. 1205 – 1214, **2004**. DOI: 10.1016/j.ijmachtools.2004.03.011

[12] Almoussawi, M. Smith, A.J. “Thermo-mechanical effect on poly crystalline boron nitride tool life during friction stir welding (dwell period)”, Metals and Materials International 24(3), pp. 560 – 575, **2018**. DOI: 10.1007/s12540-018-0074-y

[13] Sahlot, P., Jha, K., Dey, G. K., Arora, A. “Quantitative wear analysis of H13 steel tool during friction stir welding of Cu-0.8% Cr-0.1% Zr alloy”, Wear 378, pp. 82 – 89, **2017**. DOI: 10.1016/j.wear.2017.02.009

[14] Prater, T. “Friction stir welding of metal matrix composites for use in aerospace structures”, Acta Astronautica 93, pp. 366 – 373, 2014. DOI: 10.1016/j.actaastro.2013.07.023

[15] Siddiquee, A. N., Pandey, S. “Experimental investigation on deformation and wear of WC tool during friction stir welding (FSW) of stainless steel”, The International Journal of Advanced Manufacturing Technology 73(1-4), pp. 479 – 486, **2014**. DOI: 10.1007/s00170-014-5846-z

[16] Sahlot, P., Jha, K., Dey, G. K., Arora, A. “Wear-induced changes in FSW tool pin profile: effect of process parameters”, Metallurgical and Materials Transactions A 49(6), pp. 2139 – 2150, **2018**. DOI: 10.1007/s11661-018-4580-9

[17] Mastanaiah, P., Sharma, A., Reddy, G. M. “Role of hybrid tool pin profile on enhancing welding speed and mechanical properties of AA2219-T6 friction stir welds”, Journal of Materials Processing Technology 257, pp. 257 – 269, **2018**. DOI: 10.1016/j.jmatprotec.2018.03.002

[18] Banik, A., Saha, A., Barma, J. D., Acharya, U. Saha, S. C. “Determination of best tool geometry for friction stir welding of AA 6061-T6 using hybrid PCA-TOPSIS optimization method”, Measurement 173, p. 108573, **2021**. DOI: 10.1016/j.measurement.2020.108573

[19] Dialami, N., Chiumenti, M., Cervera, M., Segatori, A., Osikowicz, W. “Enhanced friction model for Friction Stir Welding (FSW) analysis: Simulation and experimental validation”, International Journal of Mechanical Sciences 133, pp. 555 – 567, 2017. DOI: 10.1016/j.ijmecsci.2017.09.022

[20] Jagadeesha, C. B. “Analysis and design of friction stir welding tool”, Journal of the Mechanical Behavior of Materials 25(5-6), pp.179 – 182, **2016**. DOI:10.1515/jmbm-2017-0006

[21] Alwin, Allawi H., Ksibi, Hatem, Driss, Zied and Alalkawi, Hussain J. M. “Fatigue Variable Loading Under Combined High Temperature and Shot Peening Treatment for AA2024-T4 and AA2024-T361”, Strojnícky časopis – Journal of Mechanical Engineering 73(1), pp. 1 – 12. 2023. DOI: 10.2478/scjme-2023-0001

[22] Moltasov, A., Tkach, P., Ustynenko, O., Protasov, R. “Effect of Misalignment of Axes in Double-Sided Weld on Stresses Distribution in Butt Welded Joints”, Strojnícky časopis – Journal of Mechanical Engineering 73(1), pp. 137 – 146, **2023**. DOI: 10.2478/scjme-2023-0011

[23] Johnsen, S. E. J., Doner, M. “A statistical simulation model of Miner’s rule”, ASME. J. Eng. Mater. Technol 103(2), pp. 112 – 117, **1981**. DOI: 10.1115/1.3224981

[24] Su, H., Wu, C. S., Pittner, A., Rethmeier, M. “Simultaneous measurement of tool torque, traverse force and axial force in friction stir welding”, Journal of Manufacturing processes 15(4), pp. 495 – 500, **2013**. DOI: 10.1016/j.jmapro.2013.09.001

[25] Pankaj, P., Tiwari, A., Biswas, P., Rao, A.G. “Plasma-Assisted Hybrid Dissimilar Friction Stir Welding for Joining of DH36 Steel and AISI 1008 Steel: Thermal Modelling and Experimental Analysis”, Arabian Journal for Science and Engineering, 46, pp.7929 – 7952, **2021**. DOI:10.1007/s13369-021-05574-y

[26] Biswas P., A Kumar D., Mandal NR. “Friction stir welding of aluminum alloy with varying tool geometry and process parameters”, Proceedings of the Institution of Mechanical Engineers, Part B: Journal of Engineering Manufacture 226(4), pp. 641 – 648, **2012**. DOI: 10.1177/0954405411424111

[27] Kumar, D. A., Biswas, P., Tikader, S, M. M. Mahapatra, N. R. Mandal. “A study on friction stir welding of 12mm thick aluminum alloy plates”, J. Marine. Sci. Appl. 12, pp. 493 – 499, 2013. DOI: 10.1007/s11804-013-1221-y